

Shear Properties of Brain Tissue Using Non-linear Green-Rivlin Viscoelastic Constitutive Equation

E. G. Takhounts, J. R. Crandall, and B. T. Matthews

ABSTRACT

Nonlinear shear properties of brain tissue were experimentally determined using an integral form of the third order Green-Rivlin constitutive equation. Overall 156 cylindrical brain specimens from 26 bovine cadaver brains were used to quantify the spatial and temporal nonlinear behavior of brain tissue. The assumptions of homogeneity, isotropy and incompressibility of brain material were made in order to reduce the required number of experiments. A series of single-, two-, and three-step strain inputs were applied to one end of a cylindrical brain specimen and stress-time histories were measured at the other end. The time delays between the applied strain step inputs were altered in order to determine the temporal nonlinearity of brain tissue. To accomplish this task a custom parallel plate experimental system was designed and built allowing high resolutions of applied displacements and time delays (0.1 mm and 0.1 s respectively). The study resulted in the nonlinear constitutive equation of brain tissue in a form of the third order integral polynomial. This equation can be subsequently implemented in any of the commercially available dynamic finite element packages to study complicated stress states resulted in brain from application of arbitrary shaped strain histories.

INTRODUCTION

The brain may be the most critical organ to protect from trauma because anatomical injuries to its structures are currently nonreversible, and the consequences of these injuries can be devastating. About 75,000 to 100,000 people die each year as a result of traumatic brain injury, which is the leading cause of death and disability in children and young adults. Data compiled by the Department of Health and Human Services (1989) indicate that someone receives a head injury every 15 seconds in the United States.

Several studies (Gennarelli, 1981; Tarriere, 1981; Chapon, *et al.* 1983) have attempted to describe the incidence and sequelae of the brain injuries. In a study conducted by Gennarelli, for example, 48% of the patients had injuries due to falls and assaults, while the remaining 52% had injuries resulting from automobile accidents (occupants and pedestrians). It was found that three out

of four automobile related brain injuries were of the diffuse type (i.e., brain swelling, concussion, and diffuse axonal injury), while one out of four were of the focal type (epidural hematomas, subdural hematomas, intracerebral hematomas and contusions). Deformation of the brain and the resulting strain, primarily shear strain, in the axonal tissue produces concussions if the injury is reversible and diffuse axonal injury if it is not reversible.

Analytical modeling of the head for the study of brain injuries has been an active field of research for many years, but the lack of knowledge of the deformation properties of brain tissue has been a weak point for all of these models. The purpose of this study was to determine experimentally the nonlinear constitutive equation for brain tissue. Shear properties of the brain material were investigated by performing single-, two- and three-step loading stress-relaxation tests. The integral polynomial form of the third order Green-Rivlin constitutive equation was applied to model nonlinear behavior of the brain tissue. The third order theory was required, in particular, to model nonlinear shear behavior known to be essentially an odd-order phenomenon.

PREVIOUS STUDIES OVERVIEW

The investigations of material properties of brain tissue has been an active field of research since the 1960's (Table 1).

Table 1: Summary Of The Previous Studies

Reference	Method	Test Subject	Shear Storage Modulus (kPa)	Shear Loss Modulus (kPa-s)
Koeneman (1966)	Creep and Oscillatory compression at 80-350Hz	Rabbit, pig and rat brain	2.7 – 5.0	0.5 – 3.2
Gafford and McElhaney (1969)	Free axial vibration at 34 Hz	Human and monkey brain	22.2	8.7
Fallenstein, Hulce and Melvin (1969a, 1969b)	Oscillatory parallel shear plates at 10 Hz and maximum strain of 0.35	White cerebral tissue of human brain	0.6 – 1.1	0.35 – 0.6
Estes and McElhaney (1970)	Dynamic compression at constant velocities up to 0.25 m/s (10 in/s)	Human and rhesus monkey brain	From 4.7 at low velocity to 18.7 at maximum velocity	N/A
Shuck and Advani (1972)	Oscillatory torsional tests at 10 – 60 Hz	Human brain tissue	8 – 15.6 for 10 – 60 Hz respectively, 7 for more than 60 Hz	3.2 – 8.6 for 10 – 60 Hz respectively, 7 for more than 60 Hz
Ljung (1975)	Transient rotary motion of a sample enclosed in a cylinder at 0.06 s duration	Human brain tissue	1.7	0.92
Donnelly and Medige (1993, 1997)	Transient single pulse high rate shear displacement	Human brain tissue	1.8	N/A
Arbogaast, Meaney and Thibault (1995)	Stress relaxation shear tests to the strain levels of 2.5 – 7.5% and strain rates of $> 1 \text{ s}^{-1}$	Porcine brainstem	2.3 for 2.5% strain and 2.9 for 7.5% strain	N/A

In Table 1 the values for shear storage and loss moduli were computed according to the following relationships:

$$\begin{aligned}
 G^* &= G' + iG'' \\
 G' &= G \\
 G'' &= \omega \xi
 \end{aligned}
 \tag{1}$$

where G^* = complex shear modulus, G' = storage modulus, G'' = loss modulus, G = elastic shear modulus, ξ = viscous constant in shear, ω = frequency.

Comparison of the results from the previous studies suggests that the material properties of the brain tissue can vary dramatically depending on the test method. For instance, the elastic storage

modulus ranges from 0.6 kPa (Fallenstein, Hulce and Melvin, 1969) to 22 kPa (Galford and McElhaney, 1969).

Most of the studies were performed using the assumption that the brain tissue behaves as a linear viscoelastic solid. This assumption may be sufficient for small deformations imposed on the material, but with increased deformations, the nonlinear behavior of brain tissue must be considered. Donnelly and Medige (1993) performed the only study in which the brain tissue was assumed to be a nonlinear viscoelastic solid. They applied 100% engineering shear strain to brain samples at different strain rates. The data was fit, however, into a material law that could not be generalized to use for arbitrary strain and strain-rate histories. A new approach was necessary to determine nonlinear properties of the brain tissue. An integral polynomial form of the third order Green-Rivlin constitutive equation was chosen to accomplish this task.

METHODS

Sample Handling And Preparation

Samples were obtained from fresh bovine brains with the age of cows ranging from two to 10 years old. Fresh bovine brain samples were obtained within twenty-four hours of death and were kept moist and refrigerated during the next twenty-four hours while experiments were performed. Access to the brain was established by cutting the upper skull of the head of the specimen using a biomedical saw (Lipshaw 230 VAC Striker Saw, Lipshaw Inc., Pittsburgh, PA 15275). The dura was cut away and the samples were excised using a custom coring tool. Approximately six samples were obtained from each bovine specimen (FIG. 1).

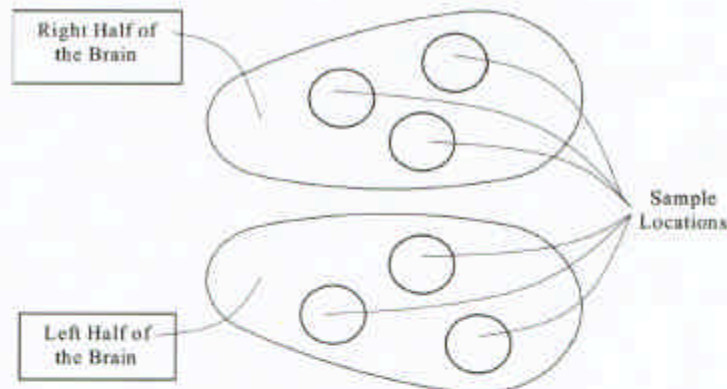


FIG. 1. Bovine brain samples location (top view)

While inside the coring tool, the ends of samples were trimmed using a scalpel with the sample moved towards the end of the core with a specially designed plunger. After trimming, the samples were transferred into glass jars filled with saline. The sample jars were labeled and refrigerated at a temperature of 4.4°C.

Dimensions of the samples were measured before testing with the samples submerged in plastic sample dishes filled with saline at room temperature. A caliper was used to measure the sample length and diameter. The length was measured twice at right angles to each other and the mean value was taken as a true length of the sample (FIG. 2). The diameter was measured four times: twice at each end at right angles. The mean value was taken as the true diameter of the sample.

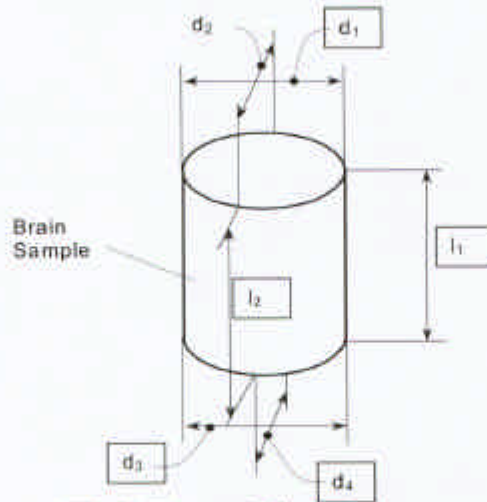


FIG. 2. The sample dimensions measurements

Test Equipment

A parallel plate experimental system, shown in FIG. 3, was designed to provide the combined measurement of shear and tensile properties of the brain tissue simultaneously. The brain sample was attached to a single axis force transducer (Sensotec Inc., Columbus, Ohio, Model 31/1435-03-04) with a full scale of 250 g and the sensitive axis located along the shear direction (FIG. 4) to measure the force response in the shear direction. The shear force transducer was in turn attached to another transducer (Sensotec, Columbus, Ohio, Model 31/1434-01-01) with a full scale of 500 g and the sensitive axis along the tensile direction. The tensile transducer was rigidly fixed on the upper shear plate. The brain sample was attached to the shear transducer using methyl-2-cyanoacrylate adhesive (Super Glue Corporation, Rancho Cucamonga, CA). The upper shear plate was bolted to the side holders with two pairs of #8-32 hex-bolts. The other end of the brain sample was glued to the lower shear plate, which was mounted on the carrier of the programmable linear actuator (NSK Ltd., Japan, Model XY-FS0060-902) with a stroke of 600 mm. The linear actuator could be programmed to move the carrier with the mounted lower shear plate to 12 different positions with an accuracy of 0.1 mm and speeds from 5 mm/sec to 400 mm/sec.

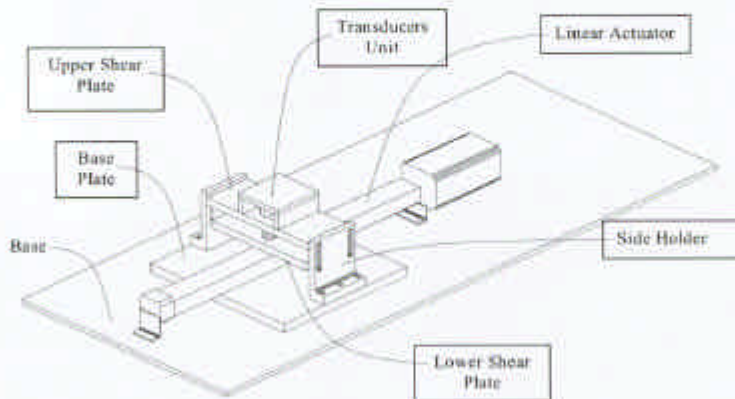


FIG. 3. A parallel plate experimental system

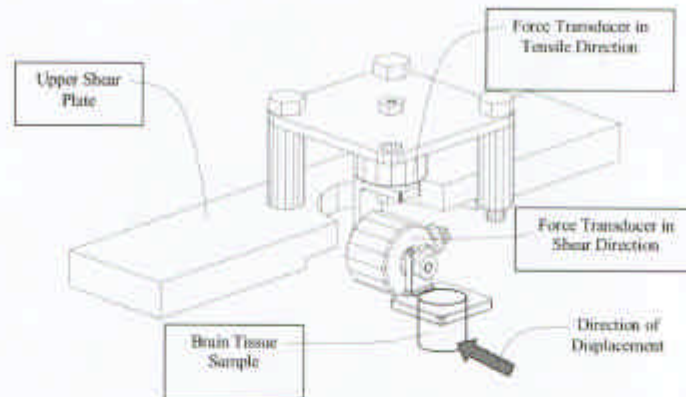


FIG. 4. Upper shear plate assembly

Time delays between step displacements were established through a custom automatic sequencer. The displacements were programmed using the teaching box (NSK Ltd., Japan, Model XY-TB1610). The In Dummy Data Acquisition System (Robert A. Denton Inc., Rochester Hills, MI) was used in these tests to collect the data at a sampling frequency of 2000 Hz and a low-pass hardware filtering frequency of 500 Hz. The data were transferred from the In Dummy Data Acquisition System (IDDAS) into an IBM compatible personal computer (Sharp Electronics Corp., Sharp Plaza, Mahwah, NJ, Model PC-3040) where they were analyzed and stored.

Testing Procedure

Samples were removed from the refrigerator and placed into a plastic container approximately two hours prior to testing to attain room temperature. The selected sample was removed from the glass jar and placed into the sample dish filled with saline solution. The dimensions of the sample were measured again, and the linear actuator was programmed using the teaching box. The sample was then placed into the coring tool and the plunger was used to support it from one end while the other end of the sample was exposed to the air from the blunt end of the coring tool. The exposed end of the sample was blotted dry with tissue and cotton swabs (Q-tips), then the adhesive was applied. Two different cyanoacrylate adhesives in the form of gel and liquid were tested for adhesion with brain tissue. The liquid form was chosen over the gel because it gave qualitatively better results. The upper shear plate unit was turned upside down so that the sample mount rigidly connected to the transducer was facing up. The cyanoacrylate adhesive was applied to the plane surface of the sample mount and the sample was pressed lightly onto it. The core was left standing in place to support the sample while the adhesive set up. After approximately three minutes, the core was removed and the sample was photographed.

Two linear rod bearings were used to set the predefined gap between lower and upper shear plates in order to set the distance between the plane surface of the cylindrical sample mount and the lower shear plate to the measured length of the sample. The rod bearing length was set according to the formula (FIG.5): $L_{rb} = L_s + L_m + L_h$.

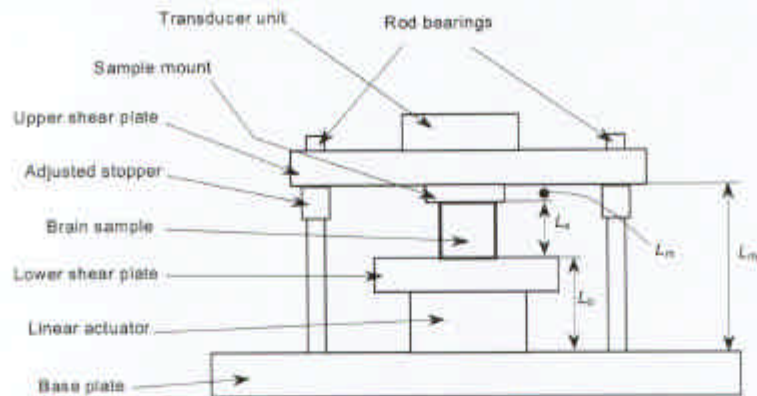


FIG. 5. The shear plate assembly with rod bearings (front view)

The cyanoacrylate adhesive was applied to the exposed end of the sample and to the lower shear plate. Two rod bearings were installed and the upper shear plate was placed above the lower shear plate so that the rod bearings would touch the base plate and four bolt threads on the side of the upper shear plate would align with the corresponding holes on the side holders to provide parallel surfaces. The upper shear plate was bolted to the side holders and the rod bearings were removed. The slight sample extension that occurred due to the sample's weight upon inversion of the assembly caused the sample to contact the lower shear plate and become slightly compressed as the plates were correctly located. The assembly was left for five minutes to allow the adhesive to cure. The displacements and time delays were applied using the automatic sequencer. The time between the final removal of the sample from the saline solution and testing was less than 30 minutes. After testing, the sample was cut away from the shear plates with a scalpel, and stored in a glass jar filled with a 10% formaldehyde solution for further histological analysis.

Assumptions

The following assumptions were made in this study: 1) Brain tissue is a viscoelastic material. Biological materials are traditionally assumed to be viscoelastic in behavior because tissue, both soft and hard, demonstrates the rate dependence and time dependence associated with viscoelastic materials. Most studies performed to date on human brain tissue have made the assumption that the brain tissue is viscoelastic in nature; 2) Brain tissue is a homogeneous and isotropic material. This analytical assumption is made for the reason of simplifying the experimental requirements; 3) The average shear stress measured at one end surface of a cylindrical sample of brain tissue corresponds to the shear strain in the central fiber of every cross section. The relationship between the average shear stress and the central fiber strain is the same as the material shear stress versus strain relationship at any point (Donnelly and Medige, 1993). In the case of a nonlinear viscoelastic material, such as brain tissue, the stress and strain distributions are unknown. Stress and strain is zero on the boundary and the strain along the centerline of the cylinder is the displacement divided by the length. However, the distributions of the stress and strain over the cross section are not linearly related. The average shear stress was *found* by measuring the reaction force in the direction of displacement of the bottom end of the sample and divided by the true cross sectional area of the stretched sample; 4) The average tensile stress measured at one end surface of a cylindrical sample of brain tissue corresponds to the strain in the central fiber of every cross section. The same considerations as in assumption 3 for shear stress and strain are valid for tensile stress and strain. The tensile stress was assumed to have negligible effect on shear stress over the tested range of strains; 5) The weight of the sample acting in the vertical direction along the axis of the cylinder has a negligible affect on the shear stress and strain (Donnelly and Medige, 1993); 6) The sample-to-sample and specimen-to-specimen variance was averaged over a large number of tests performed on the large samples. There is considerable variance

in brain tissue stress-strain properties due to: a) Material inhomogeneity and anisotropy, b) Age and gender, and c) Postmortem period prior to testing.

Although the assumptions of homogeneity and isotropy were made in the performed experiments, force measurements on different tissue samples from different locations and in different directions is most likely to be different. One way to deal with this variation was to test large samples of tissue and effectively average the varying tissue properties over the sample. These large samples contained different tissue types, fissures, vessels and membrane (pia matter), and the force measurements provided the average stress-strain properties of brain tissue. An additional advantage of this approach was that measurement of larger forces improved the signal-to-noise ratio. The assessment of variation in stress-strain properties of brain tissue due to gender, age and pre-test postmortem period would require a large number of samples, tests and subjects, which goes beyond the boundaries of this study; and 7) Brain tissue is an incompressible material. It is generally accepted that brain tissue has a bulk modulus of 2000 MPa approximately and that the shear modulus is about 10^{-5} of the bulk modulus. Thus, brain material can be considered as incompressible to simplify experimental work.

Green-Rivlin Constitutive Equation

A most general form of the third order nonlinear constitutive relation for multiaxial state of strain in terms of stress-relaxation can be written as follows (Findley *et. al.*, 1976)

$$\begin{aligned} \underline{\underline{\sigma}}(t) = & \int_0^t \mathbf{1} \left[G_1 \underline{\underline{\dot{\epsilon}}}(\tau_1) + G_2 \underline{\underline{\dot{\epsilon}}}(\tau_1) \right] d\tau_1 \\ & + \int_0^t \int_0^{\tau_1} \mathbf{1} \left[G_3 \underline{\underline{\dot{\epsilon}}}(\tau_1) \underline{\underline{\dot{\epsilon}}}(\tau_2) + G_4 \underline{\underline{\dot{\epsilon}}}(\tau_1) \underline{\underline{\dot{\epsilon}}}(\tau_2) \right] + G_5 \underline{\underline{\dot{\epsilon}}}(\tau_1) \underline{\underline{\dot{\epsilon}}}(\tau_2) + G_6 \underline{\underline{\dot{\epsilon}}}(\tau_1) \underline{\underline{\dot{\epsilon}}}(\tau_2) \Big] d\tau_1 d\tau_2 \\ & + \int_0^t \int_0^{\tau_1} \int_0^{\tau_2} \mathbf{1} \left[G_7 \underline{\underline{\dot{\epsilon}}}(\tau_1) \underline{\underline{\dot{\epsilon}}}(\tau_2) \underline{\underline{\dot{\epsilon}}}(\tau_3) + G_8 \underline{\underline{\dot{\epsilon}}}(\tau_1) \underline{\underline{\dot{\epsilon}}}(\tau_2) \underline{\underline{\dot{\epsilon}}}(\tau_3) \right] + G_9 \underline{\underline{\dot{\epsilon}}}(\tau_1) \underline{\underline{\dot{\epsilon}}}(\tau_2) \underline{\underline{\dot{\epsilon}}}(\tau_3) \\ & + G_{10} \underline{\underline{\dot{\epsilon}}}(\tau_1) \underline{\underline{\dot{\epsilon}}}(\tau_2) \underline{\underline{\dot{\epsilon}}}(\tau_3) + G_{11} \underline{\underline{\dot{\epsilon}}}(\tau_1) \underline{\underline{\dot{\epsilon}}}(\tau_2) \underline{\underline{\dot{\epsilon}}}(\tau_3) + G_{12} \underline{\underline{\dot{\epsilon}}}(\tau_1) \underline{\underline{\dot{\epsilon}}}(\tau_2) \underline{\underline{\dot{\epsilon}}}(\tau_3) \Big] d\tau_1 d\tau_2 d\tau_3, \end{aligned} \quad (1)$$

where G_1 to G_{12} are relaxation kernel functions which must be determined from experiments, and are functions of the time variables as follows:

$$\begin{aligned} G_\alpha &= G_\alpha(t - \tau_1) & \text{for } \alpha = 1, 2, \\ G_\alpha &= G_\alpha(t - \tau_1, t - \tau_2) & \text{for } \alpha = 3, 4, 5, 6, \\ G_\alpha &= G_\alpha(t - \tau_1, t - \tau_2, t - \tau_3) & \text{for } \alpha = 7, 8, 9, 10, 11, 12. \end{aligned} \quad (2)$$

G_α are symmetric with respect to their time variables.

$\overline{\underline{\underline{\dot{\epsilon}}}} = tr \underline{\underline{\dot{\epsilon}}} = \dot{\epsilon}_{ii}$ is the trace of the strain rate tensor,

$$\begin{aligned} \underline{\underline{\dot{\epsilon}}}\underline{\underline{\dot{\epsilon}}} &= \dot{\epsilon}_{ip} \dot{\epsilon}_{pj}, & i, p, j = 1, 2, 3, \\ \underline{\underline{\dot{\epsilon}}}\underline{\underline{\dot{\epsilon}}}\underline{\underline{\dot{\epsilon}}} &= \dot{\epsilon}_{ip} \dot{\epsilon}_{pq} \dot{\epsilon}_{qj}, & i, p, q, j = 1, 2, 3, \\ \overline{\underline{\underline{\dot{\epsilon}}}} &= tr(\underline{\underline{\dot{\epsilon}}}) = \dot{\epsilon}_{ii}, & i, j = 1, 2, 3, \\ \overline{\underline{\underline{\dot{\epsilon}}}\underline{\underline{\dot{\epsilon}}}} &= tr(\underline{\underline{\dot{\epsilon}}}\underline{\underline{\dot{\epsilon}}}) = \dot{\epsilon}_{ij} \dot{\epsilon}_{ji}, & i, p, j = 1, 2, 3, \\ \overline{\underline{\underline{\dot{\epsilon}}}\underline{\underline{\dot{\epsilon}}}\underline{\underline{\dot{\epsilon}}}} &= tr(\underline{\underline{\dot{\epsilon}}}\underline{\underline{\dot{\epsilon}}}\underline{\underline{\dot{\epsilon}}}) = \dot{\epsilon}_{ip} \dot{\epsilon}_{pq} \dot{\epsilon}_{qj}, & i, p, q, j = 1, 2, 3. \end{aligned} \quad (3)$$

In Eq. (1) the material was considered to be isotropic and stress and strain free prior to time zero. For incompressible material Eq. (1) reduces to

$$\begin{aligned} \underline{\sigma}(t) = \underline{s}(t) = & \int_0^t G_2 \dot{\underline{d}} d\tau_1 + \int_0^t \int_0^t G_6 \left(\dot{\underline{d}}\dot{\underline{d}} - \frac{1}{3} \mathbf{1} \dot{\underline{d}}\dot{\underline{d}} \right) d\tau_1 d\tau_2 \\ & + \int_0^t \int_0^t \int_0^t G_{12} \left(\dot{\underline{d}}\dot{\underline{d}}\dot{\underline{d}} - \frac{2}{3} \mathbf{1} \dot{\underline{d}}\dot{\underline{d}}\dot{\underline{d}} + \dot{\underline{d}}\dot{\underline{d}}\dot{\underline{d}} \right) d\tau_1 d\tau_2 d\tau_3, \end{aligned} \quad (4)$$

where the strain rate tensor $\dot{\underline{\epsilon}}(t)$ was written in terms of the deviatoric strain rate tensor $\dot{\underline{d}}(t)$ and the volumetric strain rate $\dot{\epsilon}_v(t)$

$$\dot{\underline{\epsilon}} = \dot{\underline{d}} + \mathbf{1} \dot{\epsilon}_v = \begin{vmatrix} \dot{d}_{11} + \dot{\epsilon}_v & \dot{d}_{12} & \dot{d}_{13} \\ \dot{d}_{21} & \dot{d}_{22} + \dot{\epsilon}_v & \dot{d}_{23} \\ \dot{d}_{31} & \dot{d}_{32} & \dot{d}_{33} + \dot{\epsilon}_v \end{vmatrix} \quad (5)$$

and inserted into Eq. (1).

The stress components for incompressible material in the case of pure shear

$$\dot{\underline{\epsilon}} = \begin{vmatrix} 0 & \epsilon_{12} & 0 \\ \epsilon_{21} & 0 & 0 \\ 0 & 0 & 0 \end{vmatrix} \quad (6)$$

are as follows

$$\sigma_{11}(t) = \int_0^t \int_0^t \frac{2}{3} G_6 \dot{\epsilon}_{12}^2 d\tau_1 d\tau_2, \quad (7)$$

$$\sigma_{22}(t) = \int_0^t \int_0^t \frac{2}{3} G_6 \dot{\epsilon}_{12}^2 d\tau_1 d\tau_2, \quad (8)$$

$$\sigma_{33}(t) = \int_0^t \int_0^t -\frac{2}{3} G_6 \dot{\epsilon}_{12}^2 d\tau_1 d\tau_2, \quad (9)$$

$$\sigma_{12}(t) = \int_0^t G_2 \dot{\epsilon}_{12} d\tau_1 + \int_0^t \int_0^t \int_0^t 3G_{12} \dot{\epsilon}_{12}^3 d\tau_1 d\tau_2 d\tau_3, \quad (10)$$

$$\sigma_{13} = \sigma_{23} = 0. \quad (11)$$

In this study the brain tissue was assumed to be an incompressible, homogeneous, and isotropic material. Moreover, nonlinear properties of brain tissue for pure shear condition, i.e. the material functions G_2 and G_{12} in Eq. (10) were determined. Equation (10) may be written in the following form

$$\sigma_{12}(t) = \int_0^t L_1(t-\tau_1) \dot{E}_{12}(\tau_1) d\tau_1, \quad (12)$$

$$+ \int_0^t \int_0^{\tau_1} \int_0^{\tau_2} L_3(t-\tau_1, t-\tau_2, t-\tau_3) \dot{E}_{12}(\tau_1) \dot{E}_{12}(\tau_2) \dot{E}_{12}(\tau_3) d\tau_1 d\tau_2 d\tau_3,$$

where

$$L_1(t-\tau_1) = G_2, \quad (13)$$

$$L_3(t-\tau_1, t-\tau_2, t-\tau_3) = 3G_{12}, \quad (14)$$

$\dot{E}_{12}(\tau)$ = time dependent Lagrangian shear strain.

Lagrangian strain tensor, Eq. (15), was computed from the measured dimensions of the sample and the applied shear displacement:

$$E_{ij} = \frac{1}{2} \left[\frac{\partial u_i}{\partial x_j} + \frac{\partial u_j}{\partial x_i} + \frac{\partial u_\alpha}{\partial x_i} \frac{\partial u_\alpha}{\partial x_j} \right], \quad (15)$$

where x_i is a fixed Cartesian coordinate system, u_α is a displacement vector, $u_\alpha = X_\alpha - x_\alpha$, and X_α refer to the coordinates of the deformed system. From FIG. 6:

$$u_1 = \frac{\delta}{L_0} x_2, \quad u_2 = 0, \quad u_3 = 0. \quad (16)$$

$$E_y = \begin{bmatrix} 0 & \delta/2L_0 & 0 \\ \delta/2L_0 & \delta^2/2L_0^2 & 0 \\ 0 & 0 & 0 \end{bmatrix}, \quad (17)$$

where δ is a shear displacement and L_0 is an undeformed length of the sample.

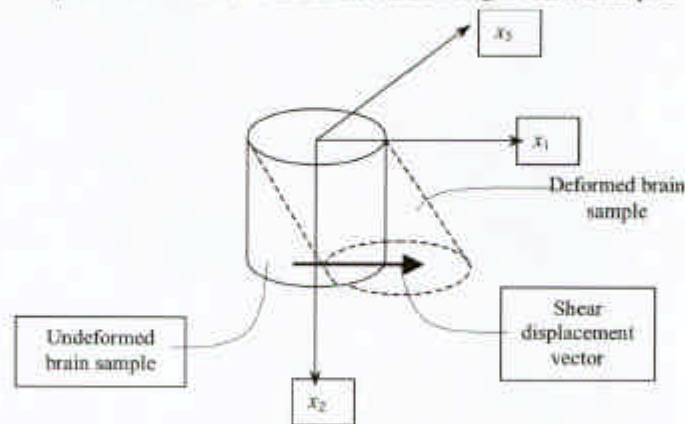


FIG. 6. Schematic of the brain sample shearing

The strain field was assumed to be uniform, i.e. each cross section along the length of the sample experienced the same shear strain. In Eq. (17) the E_{22} was assumed to be small in comparison with E_{12} so that the pure shear strain state assumption would be satisfied, and the Lagrangian strain tensor takes the following form

$$E_{ij} = \begin{bmatrix} 0 & \delta/2L_0 & 0 \\ \delta/2L_0 & 0 & 0 \\ 0 & 0 & 0 \end{bmatrix}. \quad (18)$$

The kernel functions of expressions (13) and (14) were the subject of experimental investigation.

Single-step tests

In single-step stress-relaxation tests a shear strain was applied to a cylindrical brain sample in the following form

$$P_{12}(t) = (\Delta E_{12}) H(t) \quad (19)$$

where $P_{12}(t)$ is a shear strain measure, ΔE_{12} is a constant Lagrangian shear strain, and $H(t)$ is a Heaviside step function:

$$H(t - \xi) = \begin{cases} 1 & \text{if } t \geq \xi, \\ 0 & \text{if } t < \xi. \end{cases} \quad (20)$$

The time-dependent shear stress resulting from single-step strain input was obtained by inserting Eq. (19) into Eq. (12) as follows:

$$\sigma_{12}(t) = L_1(t - \tau_1) (\Delta E_{12}) + L_3(t - \tau_1, t - \tau_1, t - \tau_1) (\Delta E_{12})^3. \quad (21)$$

Equation (21) has two unknowns: material functions $L_1(t - \tau_1)$ and $L_3(t - \tau_1, t - \tau_1, t - \tau_1)$. Therefore two single step experiments with different values ΔE_{12} were required to find these material functions. Three single step tests were performed with different values of strain ΔE_{12} (an additional test was needed to determine material function $L_3(t - \tau_1, t - \tau_2, t - \tau_3)$), and the shear stress responses were fitted to the following form of sum of exponentials

$$\sigma_{12}(t) = \sum_{i=0}^2 C_i e^{-v_i t}, \quad (22)$$

where C_i , and v_i are experimentally determined constants.

Solving system of two equations of the form (21) with two unknowns, the material functions $L_1(t - \tau_1)$ and $L_3(t - \tau_1, t - \tau_1, t - \tau_1)$ were found in the following form:

$$L_1(t - \tau_1) = \sum_{i=0}^2 C_{1i} e^{-v_{1i}(t - \tau_1)}, \quad (23)$$

$$L_3(t - \tau_1, t - \tau_1, t - \tau_1) = \sum_{i=0}^2 C_{3i} e^{-v_{3i}(t - \tau_1)}, \quad (24)$$

where C_{1i} , C_{3i} , v_{1i} , v_{3i} are computed constants.

Two-step tests

Two-step shear strain loading was applied to bovine brain samples in the form of Eq. (25) and shear stress response was measured for different combinations of times $t - \tau_1$ and $t - \tau_2$.

$$P_{12}(t) = (\Delta E_{12}^{(1)})H(t - \tau_1) + (\Delta E_{12}^{(2)})H(t - \tau_2), \quad (25)$$

where $(\Delta E_{12}^{(1)})$ is a shear strain increment applied at time τ_1 , and $(\Delta E_{12}^{(2)})$ is a shear strain increment applied at time τ_2 .

The time dependent response for the second step loading was obtained by inserting Eq. (25) into Eq. (12) as follows

$$\begin{aligned} \sigma_{12}(t) = & L_1(t - \tau_1, \Delta E_{12}^{(1)}) + L_3(t - \tau_1, t - \tau_1, t - \tau_1, \Delta E_{12}^{(1)})^2 \\ & + L_1(t - \tau_2, \Delta E_{12}^{(2)}) + L_3(t - \tau_2, t - \tau_2, t - \tau_2, \Delta E_{12}^{(2)})^2 \\ & + 3L_3(t - \tau_1, t - \tau_1, t - \tau_2, \Delta E_{12}^{(1)})^2 (\Delta E_{12}^{(2)}) \\ & + 3L_3(t - \tau_1, t - \tau_2, t - \tau_2, \Delta E_{12}^{(1)}) (\Delta E_{12}^{(2)})^2, \end{aligned} \quad (26)$$

for time $\tau_2 < t \leq \tau_3$.

where $L_3(t - \tau_1, t - \tau_1, t - \tau_2)$ and $L_3(t - \tau_1, t - \tau_2, t - \tau_2)$ are material functions to be determined from the two-step tests. All the second step shear stress responses for different times τ_2 (τ_1 was set to zero for all two step tests) were fit in the form of Eq. (22). The material functions $L_3(t - \tau_1, t - \tau_1, t - \tau_2)$ and $L_3(t - \tau_1, t - \tau_2, t - \tau_2)$ were obtained for different combinations of times τ_1 and τ_2 in the following form

$$L_3(t - \tau_1, t - \tau_1, t - \tau_2) = \sum_{j=0}^4 C_{3j} e^{-v_{3j}(t - \tau_1)} + \sum_{j=5}^{10} C_{4j} e^{-v_{4j}(t - \tau_2)} \quad (27)$$

and

$$L_3(t - \tau_1, t - \tau_2, t - \tau_2) = \sum_{j=0}^4 C_{3j} e^{-v_{3j}(t - \tau_1)} + \sum_{j=1}^6 C_{4j} e^{-v_{4j}(t - \tau_2)}.$$

Three-step tests

In three-step tests the shear strain input was used in the form of Eq. (28) and shear stress response was measured for different combinations of times $t - \tau_1$, $t - \tau_2$ and $t - \tau_3$.

$$P_{12}(t) = (\Delta E_{12}^{(1)})H(t - \tau_1) + (\Delta E_{12}^{(2)})H(t - \tau_2) + (\Delta E_{12}^{(3)})H(t - \tau_3), \quad (28)$$

where $(\Delta E_{12}^{(3)})$ is a shear strain increment applied at time τ_3 . The time dependent response for the third step loading was obtained by inserting Eq. (28) into Eq. (12) as follows

$$\begin{aligned}
\sigma_{12}(t) = & L_1(t-\tau_1, \chi \Delta E_{12}^{(1)}) + L_3(t-\tau_1, t-\tau_1, t-\tau_1, \chi \Delta E_{12}^{(1)})^3 \\
& + L_1(t-\tau_2, \chi \Delta E_{12}^{(2)}) + L_3(t-\tau_2, t-\tau_2, t-\tau_2, \chi \Delta E_{12}^{(2)})^3 \\
& + L_1(t-\tau_3, \chi \Delta E_{12}^{(3)}) + L_3(t-\tau_3, t-\tau_3, t-\tau_3, \chi \Delta E_{12}^{(3)})^3 \\
& + 3L_3(t-\tau_1, t-\tau_1, t-\tau_2, \chi \Delta E_{12}^{(1)})^2 (\Delta E_{12}^{(2)}) \\
& + 3L_3(t-\tau_1, t-\tau_2, t-\tau_2, \chi \Delta E_{12}^{(1)}) (\Delta E_{12}^{(2)})^2 \\
& + 3L_3(t-\tau_1, t-\tau_1, t-\tau_3, \chi \Delta E_{12}^{(1)})^2 (\Delta E_{12}^{(3)}) \\
& + 3L_3(t-\tau_1, t-\tau_3, t-\tau_3, \chi \Delta E_{12}^{(1)}) (\Delta E_{12}^{(3)})^2 \\
& + 3L_3(t-\tau_2, t-\tau_2, t-\tau_3, \chi \Delta E_{12}^{(2)})^2 (\Delta E_{12}^{(3)}) \\
& + 3L_3(t-\tau_2, t-\tau_3, t-\tau_3, \chi \Delta E_{12}^{(2)}) (\Delta E_{12}^{(3)})^2 \\
& + 6L_3(t-\tau_1, t-\tau_2, t-\tau_3, \chi \Delta E_{12}^{(1)}) (\Delta E_{12}^{(2)}) (\Delta E_{12}^{(3)})
\end{aligned}$$

for time $t > \tau_3$, (29)

where $L_3(t-\tau_1, t-\tau_2, t-\tau_3)$ is the material function to be determined from the three-step tests. All the third step shear stress responses for different combinations of times τ_2 and τ_3 (τ_1 was set to zero for all three-step tests) were fit in the form of Eq. (22). The material function $L_3(t-\tau_1, t-\tau_2, t-\tau_3)$ was obtained for different combinations of times τ_1, τ_2 and τ_3 in the following form

$$L_3(t-\tau_1, t-\tau_2, t-\tau_3) = \sum_{i=0}^2 C_{3i} e^{-v_{3i}(t-\tau_i)} + \sum_{j=1}^2 C_{4j} e^{-v_{4j}(t-\tau_j)} + \sum_{k=1}^{10} C_{5k} e^{-v_{5k}(t-\tau_3)}. \quad (30)$$

Function $L_3(t-\tau_1, t-\tau_2, t-\tau_3)$ was fit into several different models, but the best fit was obtained in the following form

$$L_3(t-\tau_1, t-\tau_2, t-\tau_3) = \sum_{i=0}^4 A_i e^{-v_i(3t-\tau_1-\tau_2-\tau_3)}, \quad (31)$$

where A_i are constants.

RESULTS

From single step tests the shear stress responses were obtained, and curve fitted in the form of Eq. 22, with experimentally determined constants of fit shown in Table 2.

Table 2: Experimentally Determined Constants From Single-Step Shear Tests

	C_0 (Pa)	C_1 (Pa)	C_2 (Pa)	v_1 (s ⁻¹)	v_2 (s ⁻¹)
$\Delta E_{12}=0.125$	73.794	57.437	27.960	21.739	1.370
$\Delta E_{12}=0.175$	107.042	69.863	39.362	17.189	1.247
$\Delta E_{12}=0.200$	152.734	107.315	55.808	14.916	1.047

The material functions $L_1(t - \tau_1)$ and $L_3(t - \tau_1, t - \tau_1, t - \tau_1)$ were obtained from the single step tests in the form of Eqs. 23 and 24, with the material constants presented in Table 3.

Table 3: Constants Of Material Functions $L_1(t - \tau_1)$ AND $L_3(t - \tau_1, t - \tau_1, t - \tau_1)$.

Coefficients	$L_1(t - \tau_1)$	Coefficients	$L_3(t - \tau_1, t - \tau_1, t - \tau_1)$
C_{10} , Pa	478.927	C_{30} , Pa	7118.6
C_{11} , Pa	754.039	C_{31} , Pa	-18851.0
C_{12} , Pa	-343.958	C_{32} , Pa	22013.3
C_{13} , Pa	367.059	C_{33} , Pa	-9176.48
C_{14} , Pa	-178.872	C_{34} , Pa	11447.8
ν_{11} , s ⁻¹	21.739	ν_{31} , s ⁻¹	21.739
ν_{12} , s ⁻¹	14.916	ν_{32} , s ⁻¹	14.916
ν_{13} , s ⁻¹	1.370	ν_{33} , s ⁻¹	1.370
ν_{14} , s ⁻¹	1.047	ν_{34} , s ⁻¹	1.047

Since the computed constants are representing the data points, but not the physical property of the brain material, the function $L_1(t - \tau_1)$ was refit in the form of Eq. (22) with the $R^2 = 0.999$ (Table 4).

Table 4: Relaxation And Time Constants For Material Function $L_1(t - \tau_1)$.

	$L_1(t - \tau_1)$
C_0 , Pa	476.454
C_1 , Pa	421.337
C_2 , Pa	183.208
ν_1 , s ⁻¹	-29.491
ν_2 , s ⁻¹	-1.705

From two step tests the shear stress responses for different times τ_2 were measured and fitted the form of Eq. 22 (Tables 5 and 6).

Table 5: Experimentally determined coefficients of fits of shear stress responses at different time τ_2 and applied Lagrangian shear strain increments $(\Delta E_{12}^{(1)}) = 0.125$ and $(\Delta E_{12}^{(2)}) = 0.175$.

	C_0 (Pa)	C_1 (Pa)	C_2 (Pa)	ν_1 (s ⁻¹)	ν_2 (s ⁻¹)
$\tau_2 = 0.2$ s	524.774	550.937	321.212	17.416	1.217
$\tau_2 = 0.4$ s	472.340	325.088	220.644	16.112	1.087
$\tau_2 = 0.6$ s	452.383	291.086	198.112	16.810	1.176
$\tau_2 = 0.8$ s	440.011	275.361	189.29	17.835	1.278
$\tau_2 = 1.0$ s	427.218	259.367	182.076	18.372	1.360

©

Table 6: Experimentally Determined Coefficients Of Fits Of Shear Stress Responses At Different Time τ_2 And Applied Lagrangian Shear Strain Increments $(\Delta E_{12}^{(1)})=0.125$ And $(\Delta E_{12}^{(2)})=0.2$.

	C_0 (Pa)	C_1 (Pa)	C_2 (Pa)	ν_1 (s ⁻¹)	ν_2 (s ⁻¹)
$\tau_2 = 0.2$ s	679.520	891.152	442.218	20.222	1.221
$\tau_2 = 0.4$ s	817.768	453.957	295.352	18.047	1.136
$\tau_2 = 0.6$ s	586.724	403.603	259.029	18.005	1.160
$\tau_2 = 0.8$ s	562.519	370.311	234.839	17.451	1.141
$\tau_2 = 1.0$ s	548.783	358.730	226.100	18.090	1.180

The constants of material functions $L_3(t-\tau_1, t-\tau_1, t-\tau_2)$ and $L_3(t-\tau_1, t-\tau_2, t-\tau_2)$ were obtained for different combinations of times τ_1 and τ_2 in the form of Eq. 27. The values of these constants are given in Takhounts (1998).

The three-step shear stress responses were obtained for different combinations of times τ_1 , τ_2 and τ_3 , and then curve fit in the form of Eq. 22. The coefficients of the fits for each combination of time delays are shown in Table 7.

Table 7: Experimentally Determined Coefficients Of Fits Of Shear Stress Responses At Different Combinations Of Times τ_2 And τ_3 ($\tau_1 = 0$), And Applied Lagrangian Shear Strain Increments $(\Delta E_{12}^{(1)})=0.125$, $(\Delta E_{12}^{(2)})=0.175$ And $(\Delta E_{12}^{(3)})=0.2$.

	C_0 (Pa)	C_1 (Pa)	C_2 (Pa)	ν_1 (s ⁻¹)	ν_2 (s ⁻¹)
$\tau_2 = 0.2$ s, $\tau_3 = 0.4$ s	2341.408	3411.561	1506.683	14.174	0.684
$\tau_2 = 0.2$ s, $\tau_3 = 0.6$ s	2133.4	1256.31	902.974	12.229	0.806
$\tau_2 = 0.2$ s, $\tau_3 = 0.8$ s	2027.131	1067.057	748.28	13.287	0.866
$\tau_2 = 0.2$ s, $\tau_3 = 1.0$ s	1931.782	984.554	672.913	12.567	0.809
$\tau_2 = 0.2$ s, $\tau_3 = 1.2$ s	2040.413	4034.413	1436.86	15.943	0.880
$\tau_2 = 0.4$ s, $\tau_3 = 0.8$ s	1994.771	3152.544	1338.605	14.283	0.878
$\tau_2 = 0.4$ s, $\tau_3 = 1.0$ s	1798.129	1129.926	780.792	11.814	0.738
$\tau_2 = 0.4$ s, $\tau_3 = 1.2$ s	1956.016	1349.338	889.803	13.612	0.809
$\tau_2 = 0.4$ s, $\tau_3 = 1.4$ s	1693.378	922.771	630.73	11.541	0.732
$\tau_2 = 0.6$ s, $\tau_3 = 1.2$ s	1828.226	1092.044	709.78	12.119	0.712
$\tau_2 = 0.6$ s, $\tau_3 = 1.4$ s	1635.484	850.549	573.896	12.491	0.820
$\tau_2 = 0.6$ s, $\tau_3 = 1.6$ s	1579.017	775.133	522.411	11.496	0.757
$\tau_2 = 0.8$ s, $\tau_3 = 1.6$ s	1875.332	916.0	622.558	12.816	0.842
$\tau_2 = 0.8$ s, $\tau_3 = 1.8$ s	1824.632	834.865	593.029	12.772	0.832
$\tau_2 = 1.0$ s, $\tau_3 = 2.0$ s	1555.024	730.078	501.945	12.620	0.865

The material function $L_3(t-\tau_1, t-\tau_2, t-\tau_3)$ was found in the form of Eq. 30, and then curve fit into Eq. 31 with the constants shown in Table 8.

Table 8: Constants A_i and ν_i Of Material Function $L_3(t-\tau_1, t-\tau_2, t-\tau_3)$.

A_0	A_1	A_2	A_3	A_4	ν_1	ν_2	ν_3	ν_4
7900.331	-1960.516	26098.662	-954.368	8625.135	21.739	16.225	1.370	0.920

The obtained material functions $L_1(t - \tau_1)$ and $L_3(t - \tau_1, t - \tau_2, t - \tau_3)$ can be placed into the constitutive equation (Eq. 12) which gives a nonlinear description of the material behavior in shear direction under any loading conditions:

$$\begin{aligned} \sigma_{12}(t) = & \int_0^t (476.454 + 421.337e^{-29.495(t-\tau_1)} + 183.208e^{-1.705(t-\tau_1)}) \dot{E}_{12}(\tau_1) d\tau_1 \\ & + \int_0^t \int_0^{\tau_1} \int_0^{\tau_2} (7900.331 - 1960.516e^{-21.729(3t-\tau_1-\tau_2-\tau_3)} + 26098.662e^{-16.225(3t-\tau_1-\tau_2-\tau_3)} \\ & - 954.368e^{-1.370(3t-\tau_1-\tau_2-\tau_3)} + 8625.135e^{-0.920(3t-\tau_1-\tau_2-\tau_3)}) \dot{E}_{12}(\tau_1) \dot{E}_{12}(\tau_2) \dot{E}_{12}(\tau_3) d\tau_1 d\tau_2 d\tau_3. \end{aligned} \quad (32)$$

CONCLUSIONS

Brain tissue is a nonlinear viscoelastic material.

Nonlinearity of brain tissue is spatial and temporal, i.e. linear or quasi-linear theories of viscoelasticity are not sufficient to address both types of nonlinearity.

For large deformation problems, a nonlinear constitutive equation (32) must be used. This constitutive equation is applicable to any strain history.

In the future this constitutive equation can be implemented into a finite element package such as Ls-DYNA.

ACKNOWLEDGEMENTS

This paper was sponsored in part by the American Automobile Manufacturers Association (AAMA) Agreement UVA9512-554B. The authors wish to thank Bruce Donnelly of Calspan-UB Research Center for his advice in dealing with brain material.

REFERENCES

- ARBOGAST, K. B., MEANEY, D. F., AND THIBAUT, L. E. (1995) Biomechanical Characterization of The Constitutive Relationship For The Brainstem. *Proceedings of the 39th Stapp Car Crash Conference*, P-299, pp. 153-159, Society of Automotive Engineers, New York.
- DEPARTMENT OF HEALTH AND HUMAN SERVICES (1989) Interagency Head Injury Task Force Report. National Institutes of Health, NINDS, 1-29.
- DONNELLY, B. R. AND MEDIGE, J. (1993) Shear Properties of Human Brain Tissue. Final Report No. 860, Calspan - University of Buffalo Research Center.
- DONNELLY, B. R. AND MEDIGE, J. (1997) Shear Properties of Human Brain Tissue. *J. Biomech. Engng* 119, 423-432.
- ESTES, M. S. AND MCELHANEY, J. H. (1970) Response of Brain Tissue of Compressive Loading. ASME, No. 70-BHF-13.
- FALLENSTEIN, G. T., HULCE, V. D., AND MELVIN, J. W. (1969a) Dynamic Material Properties of Human Brain Tissue. *J. Biomechanics* 2, 217-226.
- FALLENSTEIN, G. T., HULCE, V. D., AND MELVIN, J. W. (1969b) Dynamic Material Properties of Human Brain Tissue. ASME, No. 69-BHF-6.

- FINDLEY, W. N., LAY, J. S., ONARAN, K. (1976) Creep and Relaxation of Nonlinear Viscoelastic Materials With an Introduction To Linear Viscoelasticity. North-Holland publishing company, Amsterdam.
- GALFORD, J. E., AND MCELHANEY, J. H. (1969) A Viscoelastic Study of Scalp, Brain, and Dura. *J. Biomechanics* 3, 211-221.
- KOENEMAN, J. B. (1966) Viscoelastic properties of brain tissue. Unpublished M.S. Thesis, Case Institute of Technology.
- LJUNG, C. (1975) A model For Brain Deformation Due To Rotation of The Skull. *J. Biomechanics* 8, 263-274.
- TAKHOUNTS, E. G. (1998) Experimental Determination of Constitutive Equations For Human and Bovine Brain Tissue. Ph.D. thesis, UVA, Virginia.